Angle Vertex and Bisector Geometric Model for Triangular Road Sign Detection

Rachid Belaroussi and Jean-Philippe Tarel
Université Paris Est, LEPSIS, INRETS-LCPC
58, boulevard Lefebvre 75732 Paris, France
rachid.belaroussi@gmail.com http://perso.lcpc.fr/tarel.jean-philippe/

Abstract

We present a new transformation for angle vertex and bisector detection. The Vertex and Bisector Transformation (VBT) takes the image gradient as input and outputs two arrays, accumulating evidence of respectively angle vertex and angle bisector. A geometric model of the gradient orientation is implemented using a pair-wise voting scheme: normal vectors of two adjacent sides of a triangle have a specific relationship depending on the corresponding vertex angle. Our approach is able to accurately detect vertices and bisectors of a triangular road sign in a 360x270 image in about 50 ms with no particular optimization. We tested our approach on a 48 images database containing 40 triangular signs with different colors and orientations (red intersection and give way warnings, blue pedestrian crossing): 33 are correctly detected (82%) and 7 are missed with 2 false positives.

1. Introduction

Choi and Chien [5] recently presented a Corner Symmetry Transform **CST** using a bi-variate parametric model of gradient orientation inspired from the Generalized Symmetry Transform GST [12]. A vote is cast at the midpoint of two edge points, as a function of their membership to a specific angle. This membership function is computed based on the relation between the gradient orientation of these two edge points (P_i, P_j): the higher the likelihood of the points belonging to the sides of an angle, the higher the vote for their midpoint. This method leads to a biased corner detection. In our approach, a different model of corner is proposed: unlike [5], votes are not cast to midpoints of segments $[P_iP_j]$. Instead, each pair of points (P_i, P_j) with a specific gradient orientation relationship, our transform casts a vote for the corresponding angle vertex and for a set of points belonging to the angle bisector, see Fig. 1.

We apply the proposed Vertex and Bisector Transform

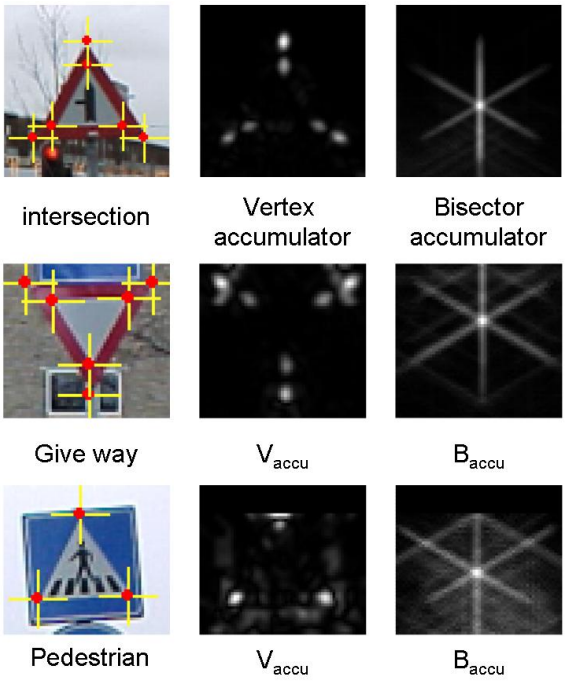

Figure 1. The three types of triangular shapes contained in the test database, with the detected vertices (yellow cross) and VBT accumulators. Red signs are made of an internal and an external triangle. Blue signs are made of an equilateral white triangle with two adjacent blue triangles. These are right triangles with only one angle in the interval $\gamma \in]\pi/6\ \pi/2[$ whose bisector can be detected in the B_{accu} accumulator.

VBT, to the detection of triangular road signs. More than a corner detector, our approach is able to detect the three vertices and their bisectors, and so the incenter of the triangle along with its spatial extent. No color model is assumed, and our approach is valid for objects with either bright/dark or dark/bright contrast, and it is robust to in-plane rotation.

In the field of traffic sign detection, most of the attention has been laid on rectangular or circular signs, especially

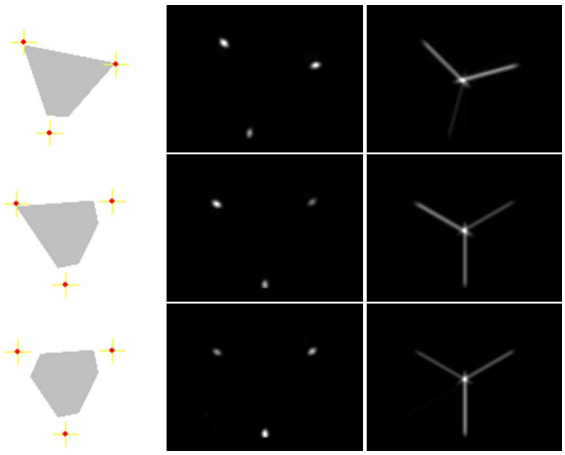

Figure 2. VBT processing of triangles with one, two and three vertex occluded. From left to right: original image with a yellow cross at detected vertex, V_{accu} vertex accumulator and B_{accu} bisector accumulator.

speed signs. A lot of approaches use signs segmentation based on a color model [7], then further process candidates with a recognition stage (genetic algorithm, PCA or template matching at several scales and positions). More interestingly, in [1] operators with automatic spatial filter selection (Adaboost) over different color representations, are used in conjunction with template matching and temporal filtering for speed signs recognition. Greyscale videos can also be processed as in [2] where the radial symmetry transform is used with the same validation steps as in [1], to detect 60 or 40 speed limitation signs. In [4], light/dark/light transitions are searched in grey level images to detect derestriction signs (a skew band in a circular speed limitation sign). A Circle Hough Transform is used to validate the presence of a circular sign around the candidates, and a temporal filtering is requested to eliminate the numerous false positives. These validation steps are not necessary with the proposed approach.

The case of triangular signs has been investigated in [11]: regions of interest are first selected based on a color threshold in the H-S plane of HSV. Straight edge chains are approximated by polygons, and under the assumption that a triangular sign is equilateral, upright and not distorted by the perspective, they search for equilateral triangle with one horizontal side and two side with a $\pm\pi/3$ radians slope. This algorithm is largely dependent on color segmentation and it is not pose-free (i.e. restricted to fronto-parallel perspective). In [10], Loy and Barnes proposed an adaptation of the radial symmetry transform **RST** for triangular signs: for each edge pixel a line of votes is cast on a perpendicular segment at a given distance. The transform is computed for a set of radii, and a final accumulator is obtained by summing over all radii. On a set of 15 images containing 15 triangular signs, their approach obtains a 100% correct detection rate with 10 false positives. A similar approach is tested more extensively in [8] for a road sign pre-detection system, but candidates are selected by a segmentation based on color threshold and morphological filters. The major drawback of the RST for triangle is that it can only recover the size and location but not orientation: it cannot distinguish a *give way* and an *intersection* panel. Our approach can precisely detect the pose of triangular road signs as their three vertices are detected, with fewer false positives than the RST is an uni-variate function of the gradient. In [6], contrarily to our approach, a colour segmentation in the H-S plane of HSI is requested. Corner detection is then used based on local binary features. Salient points detected are further clusterized as they tend to create local concentrations instead of a single corner point. Finally every combinations of triplets are checked with a constraint on the size and orientation. Performance is only measured in terms of computation time, however several examples are illustrated. A drawback of the approach is that the shape cannot be retrieved when a vertex is occluded. In Fig. 2, vertices detected by the VBT are drawn with a yellow cross, and we can see that our algorithm is robust to vertex occlusion even when the three of them are missing.

This paper is organized as follow: section 2 recalls the Generalized Symmetry Transform GST, the Corner Symmetry Transform CST and introduces the Vertex and Bisector Transform VBT. A comparison of the three transforms for the task of road sign segmentation is proposed. Experimental results are discussed in section 3, showing the VBT is orientation-independant, does not depend on light/dark or dark/light contrast, and is quite fast and efficient in outdoor environment.

2. Vertex and Bisector Geometric Model

2.1. From Generalized Symmetry Transform to Corner Detection

The Generalized Symmetry Transform **GST** [12] originally computed the symmetry magnitude between gradient orientations of two pixels (P_i, P_j) at the midpoint P of the line segment $[P_iP_j]$ joining them. For each point of the image a set of voters is defined as:

$$\Gamma_P = \{(i,j) \quad | \quad \frac{P_i + P_j}{2} = P\} \tag{1}$$

Each pixel P_i of the image has a gradient vector $\mathbf{n_i}$ with an orientation θ_i along the x-axis. Gradient vectors $(\mathbf{n_i}, \mathbf{n_j})$ at points (P_i, P_j) are directed by unit vectors. These vectors have a certain amount of radial and reflectional symmetry related to their orientation (θ_i, θ_j), computed in a two-term phase weighting function. This amount of symmetry is also weighted by a distance function decreasing with $\|\mathbf{P_iP_j}\|$, and by the magnitude of $\mathbf{n_i}$ and $\mathbf{n_j}$. Symmetry magnitude

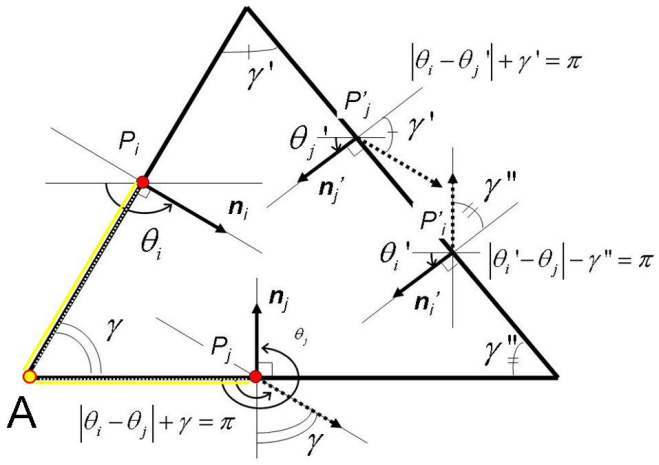

Figure 3. Gradient orientation of the sides of a triangle. The relationship between orientation θ_i and θ_j of adjacent sides depends on the corresponding angle γ, as each gradient vector $\mathbf{n_i}$ and $\mathbf{n_j}$ is orthogonal to its respective side.

at point P is the contribution of all pair of pixels in the set Γ_P:

$$S(P) = \sum_{(i,j)\in\Gamma_P} \underbrace{D(i,j)}_{\substack{\text{Distance}\\ \text{weighting}}} \underbrace{\Theta_{refl}(i,j)}_{\substack{\text{Reflectional}\\ \text{symmetry}}} \underbrace{\Theta_{rad}(i,j)}_{\substack{\text{Radial}\\ \text{symmetry}}} \underbrace{r_i\, r_j}_{\substack{\text{Gradients}\\ \text{magnitude}}} \tag{2}$$

The Corner Symmetry Transform **CST** introduced in [5], tuned this transformation to recognize symmetric features of a specific corner angle γ. The contribution of a pair of points (P_i, P_j) to the phase weighting function is made of two terms: one for reflectional symmetry and another related to their membership to the class of corners with specific angle γ. The couple (P_i, P_j) casts its vote to the midpoint P of segment $[P_iP_j]$:

$$\Theta(i,j,\gamma) = \underbrace{\Theta_{refl}(i,j)}_{\substack{\text{Reflectional}\\ \text{symmetry}}} \exp\left(-\frac{(\beta_{ij}\,(||\theta_i - \theta_j| - \pi| - \gamma))^2}{2\sigma_\gamma}\right) \tag{3}$$

The reflectional symmetry term is maximum when gradient vectors are symmetric with regards to the perpendicular bisector of segment $[P_iP_j]$. The second term of this equation has a maximum value when the corner angle $||\theta_i - \theta_j| - \pi|$ to which P_i and P_j really belong is equal to the specific angle γ. σ_γ is a parameter controlling the sensitivity of the second term. $\beta_{ij} = \left[\pi\sqrt{1-\cos^2(\theta_i - \theta_j)}\right]^{-1}$ is a rejection function ensuring that P_i and P_j do not belong to the same straight line. Finally the magnitude of the CST at point P for a specific corner angle γ is the sum of all contributions of pairs of points belonging to Γ_P:

$$S(P,\gamma) = \sum_{(i,j)\in\Gamma_P} D(i,j)\,\Theta(i,j,\gamma) r_i r_j \tag{4}$$

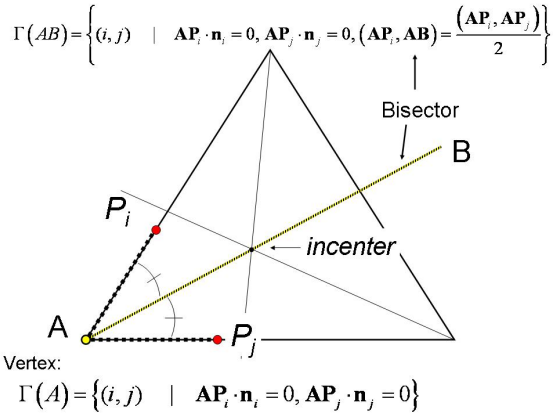

Figure 4. An angle bisector of a triangle is a straight line through a vertex which cuts the corresponding angle in half. The three angle bisectors intersect in a single point, the incenter, the center of the triangle's incircle.

One might argue that points belonging to the opposite side of an angle do not necessarily satisfy the reflectional symmetry condition as can be seen on Fig. 3. Gradients at P_i and P_j are not reflectionally symmetric vectors about their segment bisector. Therefore our approach does not use such a criterion. Also, a pair of points casts its vote to its midpoint which does not underline the corner point but a cloud of points below the corner: it is biased.

2.2. Vertex and Bisector Transformation

In our approach, a pair of edge points (P_i, P_j) casts its vote to the vertex of the corner to which they belong:

$$\Gamma(A) = \{(i,j) \quad | \quad \mathbf{AP_i} \cdot \mathbf{n_i} = 0, \quad \mathbf{AP_j} \cdot \mathbf{n_j} = 0\} \tag{5}$$

$\mathbf{n_i} = \nabla P_i = \begin{bmatrix}\frac{\partial I}{\partial x} & \frac{\partial I}{\partial y}\end{bmatrix}^T$ being the I intensity gradient at point $P_i = (x_i, y_i)$, the equation of its tangent can be deduced from its coordinates $\mathbf{n_i} = \begin{bmatrix}G_x^i & G_y^i\end{bmatrix}^T$:

$$y = a_i\,(x - x_i) + y_i \quad \text{with} \quad a_i = -\frac{G_x^i}{G_y^i} \tag{6}$$

Therefore, the vertex point A of the angle formed by the tangents to the gradient at P_i and P_j has the following coordinates:

$$\begin{cases} x_A = \frac{1}{a_i - a_j}\,(y_j - a_j x_j - y_i + a_i x_i) \\ y_A = a_i\,(x_A - x_i) + y_i \end{cases} \tag{7}$$

We also casts votes to the corresponding angle bisector, more specifically to a segment $[AB]$ defined by the vertex A and the angle $\angle P_iAB = \angle P_iAP_j/2$:

$$\begin{aligned}\Gamma(AB) = \{(i,j) \mid \mathbf{AP_i} \cdot \mathbf{n_i} = 0,\ \mathbf{AP_j} \cdot \mathbf{n_j} = 0,\\ \angle P_iAB = \angle P_iAP_j\ /2\}\end{aligned} \tag{8}$$

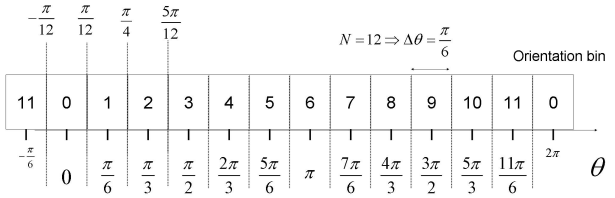

Figure 5. Gradient orientation quantization over 12 values.

The length of segment $[AB]$ depends on targets size: we set it to L_{max} the maximum size of a road sign. Now a vertex magnitude map can be build as for the GST:

$$V_{accu}(A) = \sum_{(i,j)\in\Gamma(A)} D\left(i,j\right)\Theta(i,j) r_i\, r_j \qquad (9)$$

with

$$D(i,j) = W_{L_{max}}(\|P_i - P_j\|) \qquad (10)$$

where W_R is a top-hat function with a length R:

$$W_R(x) = 1 \quad \text{if} \quad |x| < R, \quad 0 \quad \text{elsewhere} \qquad (11)$$

so that pixels too far apart cannot form a pair of voters. It is classical to choose for r_i and r_j a logarithmic function of gradient magnitude:

$$r_i = \log\left(1 + \|\nabla P_i\|\right) \quad \text{and} \quad r_j = \log\left(1 + \|\nabla P_j\|\right) \qquad (12)$$

If no specific angle shall be found, the phase function can be set as:

$$\Theta(i,j) = \Theta_{//}(i,j) = 1 - \delta\left(\cos\left(\theta_i - \alpha_{ij}\right)\right) \qquad (13)$$

where $\alpha_{ij} = \angle\left(O\mathbf{x}, \mathbf{P_i P_j}\right)$ is the angle between $\mathbf{P_i P_j}$ and the x-axis, and δ the Kronecker symbol (Dirac function). The $\Theta_{//}(i,j)$ function rejects cases where $|\theta_i - \alpha_{ij}| = \pi/2 \bmod \pi$ corresponding to a corner angle of 0 or π (P_i and P_j then being on parallel edges). Local maxima of the V_{accu} array are good candidates for angle vertices. The corresponding angle bisector magnitude is build by casting votes through segments $[AB]$:

$$B_{accu}([AB]) = \sum_{(i,j)\in\Gamma(AB)} D\left(i,j\right)\Theta(i,j) r_i r_j \qquad (14)$$

Angle bisector candidates appear as portions of line in the B_{accu} array. If a triangular shape is present in the image, its incenter is a local maxima of the B_{accu} accumulator because the three angle bisectors intersect at this point as shown by Fig. 4.

2.3. Triangular Sign Detection

In the case of triangular road signs some basic assumptions lead us to define a more specific phase weighting function $\Theta(i,j)$. Let us assume for a moment that we are looking for equilateral triangles: the base angle is $\gamma_0 = \pi/3$.

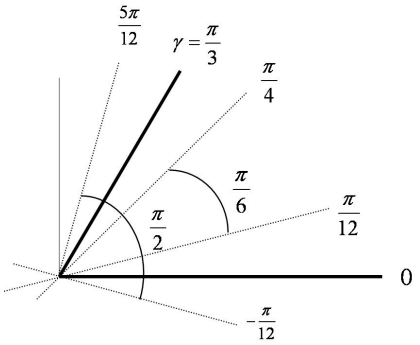

Figure 6. Orientation accuracy.

Now if the gradient orientation is quantized on N=12 values, the sample step is $\Delta\theta = \pi/6$, as shown in Fig. 5. The angle between two sides is estimated with this accuracy: the sampled value of γ_0 actually corresponds to an angle $\gamma = \pi/3 \pm \pi/6$ (before sampling).

That is to say that a model of an angle of $\gamma_0 = \pi/3$ also encapsulates angles $\gamma \in \left]\frac{\pi}{6}\ \frac{\pi}{2}\right[$, as shown in Fig. 6. For example a segment with a $-\pi/12$ angle on the x-axis would be quantified as an horizontal line, while a side with angle of $5\pi/12 - \epsilon$ would be quantified as a line with a $\pi/3$ slope so that the angle between these two lines would be quantified as $\pi/3$ instead of $\pi/2 - \epsilon$.

Now a triangular road sign projection in the image plane depends on its pose in the camera frame: it is generally a scalene triangle but the interval $\gamma \in \left]\frac{\pi}{6}\ \frac{\pi}{2}\right[$ regroups a large spectrum of camera perspectives. One can make a sharper quantization if some *a priori* knowledge about the angle to be detected is available: $\gamma = \gamma_0 \pm \frac{2\pi}{N}$ with $\gamma_0 = \frac{2k\pi}{N}$.

In order to model the specific angle $\gamma_0 = \pi/3$, the phase weighting function is designed to select only those pairs of edge points belonging to adjacent sides of a $\pi/3$ angle:

$$\Theta(i,j) = \Theta_{//}(i,j)\left(\underbrace{W_{\frac{2\pi}{N}}\left(|\theta_i - \theta_j| - \pi - \gamma_0\right)}_{\text{acute angle}} + \underbrace{W_{\frac{2\pi}{N}}\left(|\theta_i - \theta_j| - \pi + \gamma_0\right)}_{\text{obtuse angle}}\right) \qquad (15)$$

with N=12 in our experiments and $\gamma_0 = \pi/3$ as discussed earlier. The width of the top hat kernel W is $\Delta\theta = \frac{2\pi}{N}$ which ensures that numerically $|\theta_i - \theta_j| - \pi = \gamma_0$ or $-\gamma_0$: these two cases are illustrated in Fig. 3.

Two accumulators are available: our strategy to detect a triangle is first to detect incenters using B_{accu}, then to associate each of them to a triplet of vertices using V_{accu}. An incenter is detected by looking for local maxima of B_{accu} above a threshold τ_0. We seek in V_{accu} for the closest higher

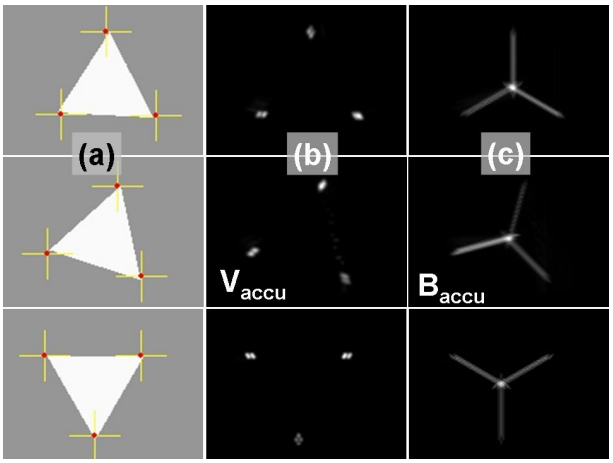

Figure 7. Column (a): source image with detected vertex in yellow. (b): V_{accu} vertex accumulator. (c): B_{accu} accumulator showing bisector magnitude.

Images	Targets	True Pos.	False Pos.	Process. Time
48	40	33 (82.5%)	2	<50 ms/img

Table 1. Road sign detection performance on a 48 urban images for two fixed thresholds τ_0 on B_{accu} and τ_1 on V_{accu}.

local maxima above a second threshold τ_1. If a local maximum of B_{accu} is associated with three vertices, they are respectively the incenter and vertices of a triangle.

3. Experimental Results

3.1. Illustration on synthetic images

We have illustrated the results of the transformation on some synthetic images, with both accumulators and the detected vertices. On Fig. 7, some light/dark triangles are shown whereas Fig. 9 shows objects with dark/light contrast. In both cases we can see that the transformation is almost invariant to in-plane rotation. The VBT is also robust to vertex occlusion as shown in Fig. 2. Indeed, set of voters are taken from the sides of a triangle so if a consistent portion of the triangle edges is still visible, its vertices can be found even if they are occluded. The sensitivity to occlusion has still to be quantified, and it is a work in progress.

3.2. Triangular Road Sign Detection

We have tested our approach on the traffic sign image database [9]. It is a set of 48 images of size 360x270 pixels containing 37 blue signs (cycle, pedestrian) and 18 red signs (intersection, give way). Among these 55 road signs, 15 are circular and 40 contain a triangular shape which can be divided into three categories illustrated by Fig. 1:

- pedestrian crossing: a white triangle inside a blue rectangular panel,
- intersection warning: a white triangle with a pictogram inside a red triangle, with a bottom side horizontal and a vertex at top,
- give way warning: a white triangle inside a red one with a vertex at the bottom and a horizontal side at the top.

Our approach is able to correctly detect 33 signs out of 40 with 2 false positives in less than 50 ms/frame on a standard PIV@1.2GHz, as summarized in Tab. 1. A road sign is detected if its three vertices are detected and associated to the same incenter in B_{accu}.

Some examples are given in Fig. 8: it is interesting to see that both interior and exterior triangles vertices at the border of red signs are correctly detected. As a matter of fact, a red sign contains a total of 6 triangle vertices, whereas a blue sign contains only 3. Tab. 2 details the performance of vertices detection for these three categories.

4. Conclusion and Perspectives

We have presented a new transform for the simultaneous detection of angle vertex and angle bisector, without using any color model and even when they are occluded. It can process efficiently a 360x270 image in less than 50 ms and has been applied to triangular road sign detection. It has a high detection rate with 33 signs out of 40 correctly detected with 2 false positives on a database of 48 images. We are investigating an improved post-processing strategy to detect triangles, that combines the vertex and the bisector accumulators. Our strategy for the other polygonal and circular signs, is described in [3]. This work will be used as an automatic segmentation tools for labelling road scene images[1] and for a road sign pre-detection software.

References

[1] C. Bahlmann, Y. Zhu, V. Ramesh, M. Pellkofer, and T. Koehler. A system for traffic sign detection, tracking, and recognition using color, shape, and motion information. In *Proceedings of IEEE Intelligent Vehicles Symposium*, pages 255–260, 2005.

[2] N. Barnes and A. Zelinsky. Real-time speed sign detection using the radial symmetry detector. *IEEE Transactions on Intelligent Transportation Systems*, 9(2):322–332, 2008.

[3] R. Belaroussi and J.-P. Tarel. A real-time road sign detection using bilateral chinese transform. In *Proceedings of International Symposium on Visual Computing ISVC*, pages 1161–1170, 2009.

[1]This work is a part of the iTowns-MDCO project funded by French National Research Agency and Cap Digital

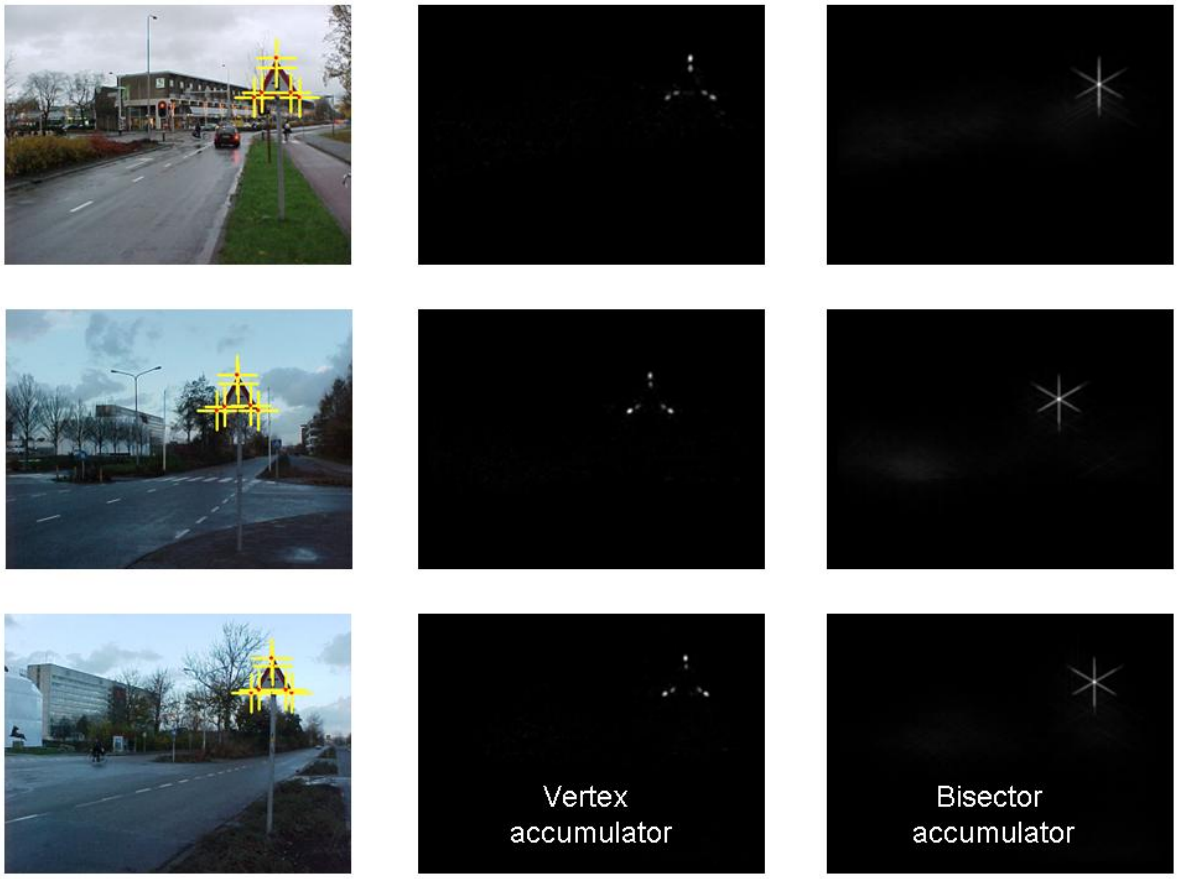

Figure 8. Examples of triangular signs detection from the traffic sign image database.

Triangular road signs	Num. of vertices	Missed vertices	Detection rate	False Positives
21 blue	63	10	84%	16
19 internal red	57	7	88%	
19 external red	57	7	88%	

Table 2. Vertex detection performance on 48 urban images, for the same threshold τ_1 on V_{accu} as in Tab. 1.

[4] C. Caraffi, , E. Cardarelli, P. Medici, P. P. Porta, G. Ghisio, and G. Monchiero. An algorithm for italian de-restriction signs detection. In *Proceedings of IEEE Intelligent Vehicles Symposium*, pages 834–840, 2005.

[5] I. Choi and S.-I. Chien. A generalized symmetry transform with selective attention capability for specific corner angles. *IEEE Signal Processing Letters*, 11(2):255–257, 2004.

[6] B. Cyganek. Real-time detection of the triangular and rectangular shape road signs. In *Proceedings of Advanced Concepts for Intelligent Vision Systems ACIVS*, pages 744–755, 2007.

[7] A. de la Escalera, J. M. Armingol, and M. Mata. Traffic sign recognition and analysis for intelligent vehicles. *Image and Vision Computing*, 21(3):247–258, 2003.

[8] P. Foucher, , P. Charbonnier, and H. Kebbous. Evaluation of a road sign pre-detection system by image analysis. In *Proceedings of International Conference on Computer Vision Theory and Applications VISAPP*, pages 362–367, 2009.

[9] C. Grigorescu and N. Petkov. Distance sets for shape filters and shape recognition. *IEEE Trans. on Image Processing*, 12(10):1274–1286, 2003.

[10] G. Loy and N. Barnes. Fast shape-based road sign detection for a driver assistance system. In *Proceedings of Intelligent Robots and Systems IROS*, pages 70–75, 2004.

[11] G. Piccioli, E. D. Micheli, P. Parodi, and M. Campani. Robust method for road sign detection and recognition. *Image Vision Computing*, 14(1):234–778, 2004.

[12] D. Reisfeld, H. Wolfson, and Y. Yeshurun. Context free attentional operators: the generalized symmetry transform. *International Journal of Computer Vision, Special Issue on Qualitative Vision*, 14(2):119–130, 1995.

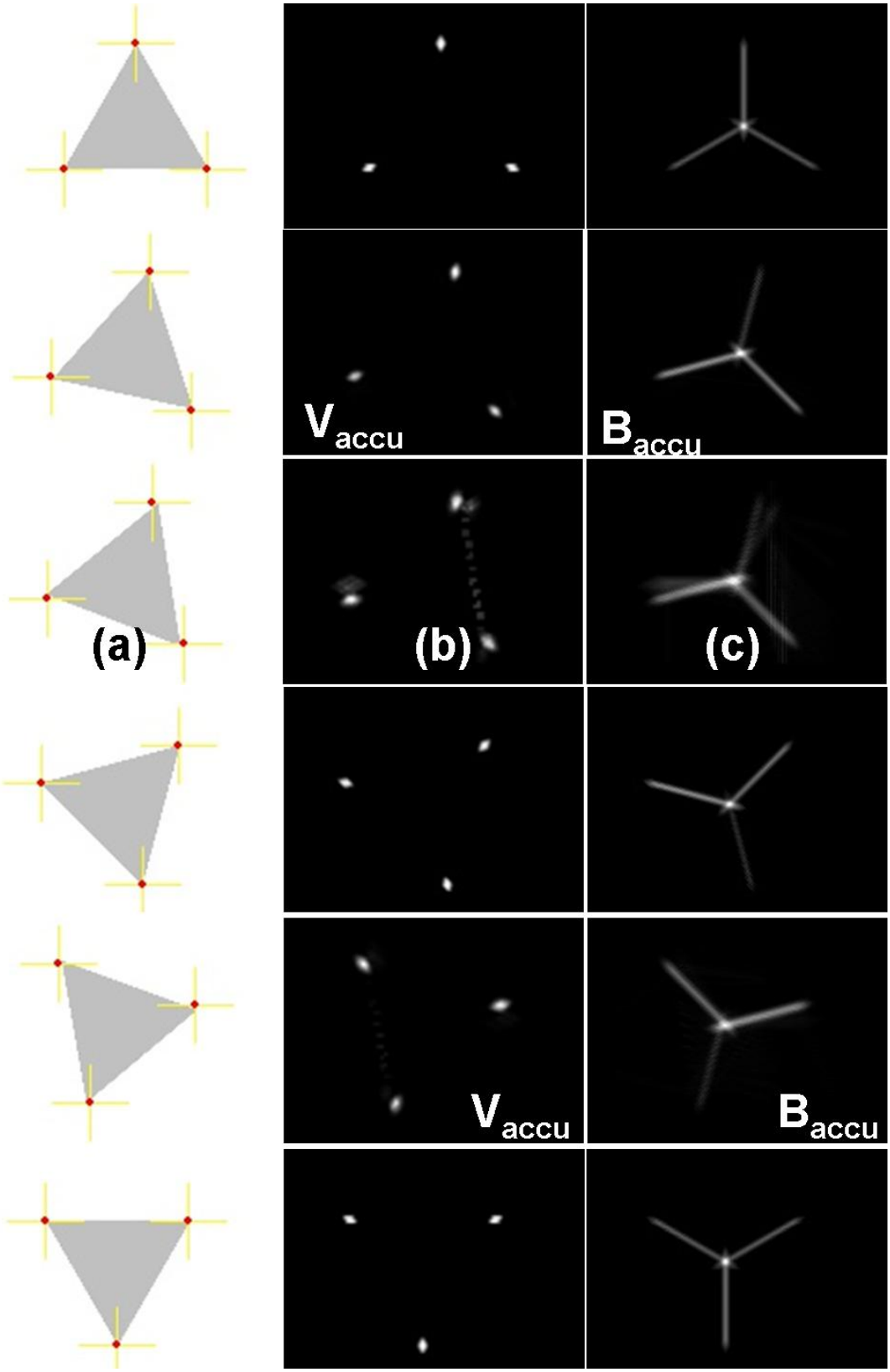

Figure 9. Examples of triangles with dark/light contrast, and different orientation. The Vertex and Bisector Transformation shows a relative invariance to in-plane rotation.